Journal of Infection and Public Health 18 (2025) 102771

Contents lists available at ScienceDirect

Journal of Infection and Public Health

journal homepage: www.elsevier.com/locate/jiph

Original article

The spread of the Delta variant in Catalonia during summer 2021: Modelling and interpretation

Benjamin Steinegger [a], Giulio Burgio [a], Piergiorgio Castioni [a,b], Clara Granell [a], Alex Arenas [a,*]

[a] Departament d'Enginyeria Informàtica i Matemàtiques, Universitat Rovira i Virgili, Tarragona 43007, Spain
[b] Barcelona Supercomputing Center (BSC), Barcelona, Spain

ARTICLE INFO

Article history:
Received 19 December 2024
Received in revised form 5 March 2025
Accepted 9 April 2025

Keywords:
COVID-19
Delta variant
Human behavior
Epidemic drivers
Infectious disease modelling

ABSTRACT

Background: The emergence of highly transmissible SARS-CoV-2 variants has posed significant challenges to public health efforts worldwide. During the summer of 2021, the Delta variant (B.1.617.2) rapidly displaced the Alpha variant (B.1.1.7) in Catalonia, Spain, leading to a resurgence in infections despite ongoing vaccination campaigns. Understanding the epidemiological drivers of this outbreak is critical for refining future mitigation strategies.

Methods: We employed a Bayesian age-stratified epidemiological model, incorporating vaccination status and variant-specific transmission dynamics, to analyze the outbreak in Catalonia. The model was calibrated using daily reported cases, hospitalizations, sequencing data, and vaccination coverage across age groups. We inferred contact patterns dynamically to assess their role in the epidemic resurgence and estimated the transmission advantage of the Delta variant over Alpha.

Results: Our analysis revealed that increased social interactions among younger, less vaccinated populations significantly contributed to the surge in infections. The long weekend of Sant Joan (June 23–24) coincided with a peak in contact rates, driving a rise in the reproduction number, particularly among individuals aged 20–29. We estimated that the Delta variant had a 40–60.

Conclusions: Our findings underscore the critical role of vaccination coverage in mitigating the impact of emerging variants. The combination of increased social interactions and uneven vaccine distribution exacerbated the Delta-driven resurgence. NPIs alone proved insufficient in controlling transmission, highlighting the necessity of targeted vaccination strategies to achieve robust epidemic control. This study provides a framework for assessing future variant-specific threats and informing tailored public health interventions.

Introduction

Following the emergence of SARS-CoV-2 in late 2019 [2], significant outbreaks occurred throughout the world during the spring of 2020 [3–5]. The large number of infections contributed to the development of new, more transmissible variants of concern (VOC) [6]. An example is the Alpha variant (B.1.1.7.) [7–9], which led to a considerable death toll in the United Kingdom during the winter of 2020–2021 [10]. Exactly as had already happened with the wild-type virus [11,12], the Alpha variant and other VOCs quickly spread to numerous countries and eventually replaced the original one [13]. Likewise, the Delta variant (B.1.617.2) started to replace the Alpha variant across European countries by early summer 2021 [14], due to its higher transmissibility [15–19].

In the initial stages of the pandemic, when vaccines were not yet available, aggressive non-pharmaceutical interventions (NPIs) were the only tool against the spread of the virus and its variants [15,20–22]. Only in late 2020, with the introduction of effective vaccines [23], could the majority of western countries start to relax some of their harshest policies and go back to a pre-pandemic level of social interactions. However, the question of when and how to execute the various steps towards total normalcy was plagued by several unknown factors, such as the large heterogeneity of vaccination levels across age groups, the poor estimates of vaccine efficacy against the VOC and the uncertain behavioral response of the population [18,24,25].

Catalonia, one of the most populated regions of Spain, gives us a good example of how an early NPI lift combined with the emergence

* Corresponding author.
E-mail address: alexandre.arenas@urv.cat (A. Arenas).

https://doi.org/10.1016/j.jiph.2025.102771

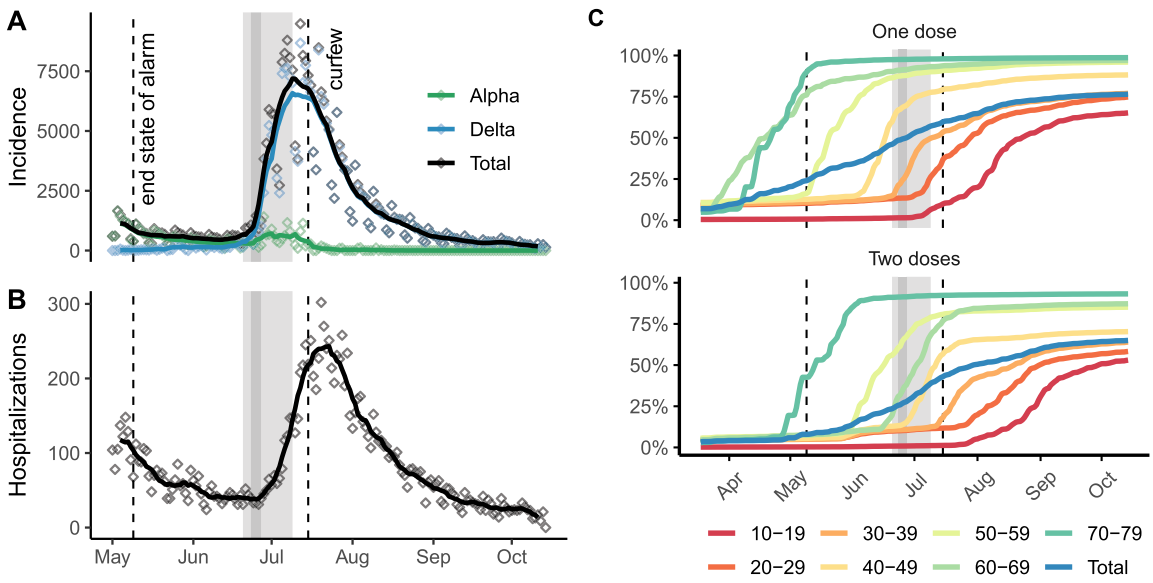

Fig. 1. Case numbers and vaccination in Catalonia. A. Daily incidence from May 1 onward is shown, with solid lines representing a 7-day centered rolling average. The daily incidence is further divided into cases attributed to the Alpha and Delta variants. Dashed lines mark the end of the state of alarm and the introduction of a curfew from 1 a.m. to 6 a.m. The grey shaded area corresponds to the period between June 21 and July 9, during which nightclubs were open. The dark grey shaded area highlights the long weekend of Sant Joan. B. Daily hospitalizations from May 1 onward. C. Evolution of the proportion of vaccinated individuals across different age groups. The data reveals that when nightclubs reopened (grey shaded area), only individuals over 50 years old had significant protection from vaccination. Vaccination for the 30–39 age group began almost simultaneously with the reopening of nightclubs. The 0–9 age group was excluded since no vaccines were administered to this group.

of the Delta variant and a relatively low vaccination levels (Fig. 1C), led to a rapid increase in the number of infections and put a massive stress on the health care system between July and August 2021 (Fig. 1A-B). As case numbers had begun to decline following the conclusion of the national state of alarm on May 9, a decision was made to reopen all local nightclubs starting on June 21 [26]. Furthermore on June 23 the regional festivities of “Sant Joan” were celebrated. This event, which includes musical performances, fireworks and large gatherings of people in the public spaces, is a tradition celebrated in many Catalan speaking regions like Catalonia and Valencia [27]. The celebrations primarily take place on the evening of June 23 and June 24 is a public holiday, and since it fell on a Thursday it is likely that many individuals used the opportunity to enjoy a long weekend. Eventually, the worrying rise in reported cases and hospitalizations led the regional health authorities to reintroduce some restrictions, like the closure of night clubs on the 9th of July and a curfew on the 15th of the same month. The curfew was subsequently overturned by the court on August 19, and nightclubs reopened on October 8 with a requirement for a vaccination certificate to enter.

The aim of this work is to understand and explain the causes that led to the aforementioned resurgence in cases. We achieve that by using an age-stratified model calibrated on the available epidemiological data, which allows us to identify the drivers behind the crisis. The model includes the time-varying vaccination coverage in the different age strata, as well as the presence of both the Alpha and the Delta variants. We then use a Bayesian framework to infer the number of contacts among different age groups throughout time. The results all point to a sharp increase in both the contact rates and the reproduction number in correspondence of the weekend of Sant Joan. The increase in infections was further exacerbated by the low vaccination coverage in the younger age groups during this period. This conclusion comes from the fact that, when the social interactions started to increase again after the lift of the curfew, that did not lead to another rise in the reproduction number, most likely due to the increased vaccination levels. Finally, making use of sequencing data, we are able to estimate the transmission advantage of the Delta variant, confirming previous estimates.

Materials and methods

Epidemiological model

We use an age-stratified compartmental model, with age groups from 0 to 80 years by steps of 10 years. We decided to exclude the 80+ age class because a detailed description in that case would required the inclusion of care homes in the dynamics, for which the necessary data is hard to find [22,28]. However, since this work is about the drivers of the epidemic rather than the negative outcomes, we think that such an exclusion will not undermine our findings. Furthermore, there are two copies of each infectious compartment in the model in order to deal with both the Alpha and Delta variant. Finally, the model classifies individuals according to their vaccination status, which can either be non vaccinated or vaccinated with one or two doses. We do not keep track of different types of vaccines due to lack of data.

Parametrization of the model

The number of people per age group is taken directly from publicly available census data, while the values of the mixing rates among them (i.e. the contact matrix) comes from Prem et al. [28] and are assumed to be constant. The hospitalization risk after an infection is informed from Knock et al. [22]. The increase hospitalization risks of the Alpha and Delta variants with respect to the wild-type are set to 1.42 [29] and 1.85 [30], respectively. Relative age differences in the risk of ICU events (admissions or deaths) are fixed [22], while the absolute values are left as a free parameters. The model also takes as input the daily number of newly vaccinated individuals in each age strata. Reduction in transmissibility and susceptibility against the Alpha and Delta variants after one or two doses are fixed. The transmission advantage of the Delta variant is left as a free parameter. Furthermore, through the comparison with the epidemiological data, we infer the day by day evolution of the contact rate of each age group.

Sequencing data

The sequencing data comes from Sistema de Notificació Microbiològica de Catalunya (SNMC) and it contains the number of daily complete sequence analyses and the detected variants for every single day. On average, 50 sequences were analyzed per day. While variants other than the Alpha and Delta were present, they only accounted for the 6 % of cases and therefore we decided to exclude them from the analysis.

Inference framework

We calibrate the model using daily numbers of infections, hospitalizations, ICU admissions and deaths. The data is age-stratified in all cases except that for ICU admissions, due to its small number. In the case of infections, we assume the detection rate to be lower than 100 % and to vary across age groups, while staying constant in time throughout the simulation. Finally, we adjust the model to match the percentage of the Delta variant detected over time, based on the sequencing data. We begin to fit model from May 1st, but in order to properly initialize it and fill all the compartments the simulation runs from April 1st. We assume a gaussian prior for the interaction rates in order to prevent overfitting. The model is calibrated within a bayesian framework. We implemented the inference in Stan [31] and run the simulation through rstan [32]. We ran four chains with 2000 steps each, 1000 of which were used for warm-up. Gelman-Rubin convergence statistics [33], i.e. potential scale reduction factors, were all smaller than 1.01. A link to the full code used for the calibration of the model can be found in the code availability statement (Table 1).

Calculation of the reproduction number

We calculate the daily reproduction number of the i-th age group through the number of secondary infections caused by an average, infected individual in age-strata i at time t. The final value will then be a weighted average of the contribution of both variants, using their relative incidence as weight. To then calculate the reproduction number for the whole population we weight the contribution of each age group with respect to its overall incidence [34]. We also estimate the reproduction number from the reported cases using EpiEstim [35,36], assuming the same generation time as used in the model. The generation time in the model is derived following Svensson's approach [37]. To infer infection times [38], we deconvolute the time series of reported cases by considering the time between infection and detection in the model, using a maximum likelihood method [39,40].

Sensitivity analysis

Our sensitivity analysis focuses on three major points. First, we take into consideration different generation times to study how they affect the estimation of the transmissibility advantage of the Delta variant. We find that it varies between 40 % and 60 %. Second, we change the relative severity of Delta variant with respect to the Alpha variant. This significantly reduces the attack rate of the age strata 20–29. Third, we show that incorporating previous infection induced immunity does not lead to major changes in the conclusions.

Table 1
Number of people per age group.

Age group	Number of people
0–9	733,902
10–19	817,128
20–29	817,128
30–39	991,146
40–49	1,271,088
50–59	1,059,240
60–69	817,128
70–79	620,412

This table summarizes the absolute number of people for each decade between 0–9 and 70–79. The 80+ class is excluded from the analysis and therefore not shown.

Results

Fig. 2 illustrates how the model aligns with the data for reported cases (A), hospitalizations (B), ICU admissions (D), and fatalities (E). Age-specific comparisons for reported cases and hospitalizations are provided in Figs. S2-S3 in the SI. Overall, the model shows strong agreement with the observed data. We estimate the Delta variant's transmission advantage to be 1.52 (CrI: 1.50–1.54). The relationship between the transmission advantage and the assumed generation time is detailed in Fig. S6 in the SI. On April 1st, the start of the simulation, the estimated number of active Delta variant cases was 53 (CrI: 37–75). The fit of the model to sequencing data is shown in Fig. 2A. The Delta variant had already become dominant by the time night clubs reopened in Catalonia (indicated by the grey shaded area). This coincided with the relatively low protection provided by vaccination, as inferred from the model. In the night clubs reopening period, we estimate that approximately 90 % of infections affected unvaccinated individuals (Fig. 2F).

Alongside the growing prevalence of the Delta variant and low vaccination coverage, we identify a sharp rise in interaction rates among younger individuals in the age groups 10–19, 20–29 and 30–39 (Fig. 3A). In these groups, the number of contacts shows a steady increase starting in early June, peaking during the long weekend of Sant Joan (indicated by the dark-grey shaded area). Notably, the 20–29 age group exhibits the most significant rise in social interactions. Following Sant Joan, interaction rates rapidly decline, even before night clubs were closed and a curfew was imposed. By contrast, age groups 40–49 and 50–59, as well as 0–9, 60–69, and 70–79 (Fig. S4 in the SI), do not exhibit any major increase in contacts around the same period. However, from mid-July onward, a rise in contact rates becomes apparent across nearly all age groups.

This subsequent generalized increase in interaction rates did not lead to a significant rise in age-specific reproduction numbers (Fig. 3B). The rollout of vaccines, particularly among younger age groups, effectively mitigated the impact of rising contact rates on the epidemic's progression. In contrast, during the earlier peak in interaction rates among the 10–19, 20–29, and 30–39 age groups, a marked spike in reproduction numbers was observed as well. In particular, the 20–29 age group reached a reproduction number of 5.0 (CrI: 4.2–5.9). The reason behind this is to be found, once again, in the limited number of vaccine doses that had been administered in these age groups (Fig. 1B), which provided the population with an insufficient level of protection during this period.

The trend of the overall reproduction number highlights the extent to which the epidemic dynamics were driven by younger age groups (Fig. 4A). Similar to the contact rates, the reproduction number reaches its peak during the long weekend of Sant Joan, with a maximum value of 3.4 (CrI: 3.0–3.9). The reproduction number inferred from the model shows good qualitative agreement with the one estimated directly from reported cases using EpiEstim (Fig. 4A). The earlier increase and subsequent decline in the reproduction number seen in the model likely result from the Gaussian smoothing prior assumed for the interaction rates (see Materials and methods). Additionally, only a small further decrease is observed following the closure of night clubs, and no significant effect is attributed to the introduction of the curfew.

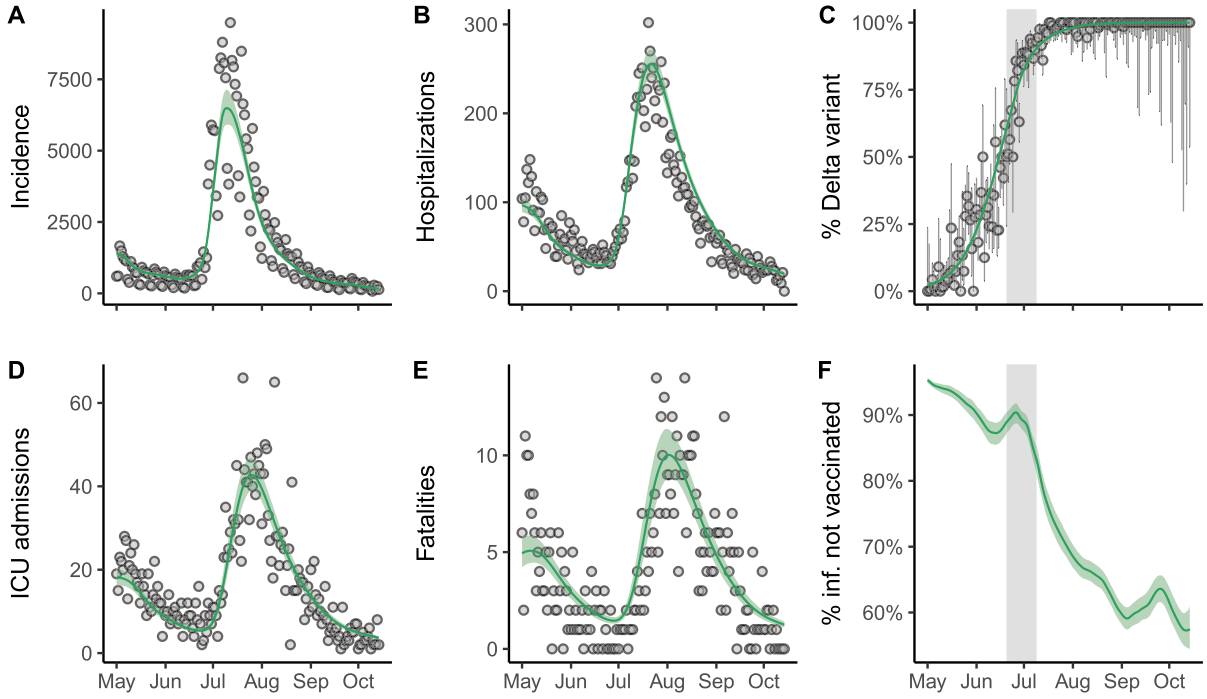

Fig. 2. Adjustment to the data. Adjustments made to the data for daily incidence (A), hospitalizations (B), ICU admissions (D), and fatalities (E) are shown. Panel C compares sequencing data with the model, depicting the fraction of infections attributed to the Delta variant. Vertical bars represent the 95 % credible interval under the assumption of a uniform prior. (F) Fraction of infected individuals who were unvaccinated. The low vaccination coverage at the time of nightlife reopening (grey shaded area) resulted in a high proportion of infections occurring among unvaccinated individuals during that period.

The detection rate varies significantly across different age groups (Fig. 4C). For the 0–9 age group, it is nearly 100 %. The age-specific IHR we use is based on data from the first and second waves in England in 2020. It is possible that increased experience in managing COVID-19 infections in young children reduced the number of precautionary hospitalizations. Another option may be that the heightened virulence of the Alpha and Delta variants compared to the wild type might not affect young children as strongly. A similar observation applies to the 70–79 age group. We estimate the lowest detection rate for the 20–29 age group at 21 % (CrI: 19–24 %). For the 10–19 age group, a slightly higher detection rate of 30 % (CrI: 25–36 %) is likely due to school protocols implemented in case of infections among the students. The age-specific heterogeneity of the detection rates, combined with changes in interaction rates, causes the overall detection rate to fluctuate over time (Fig. 4B). On May 1st, we find a detection rate of 38 % (CrI: 36–41 %), which declines to 29 %

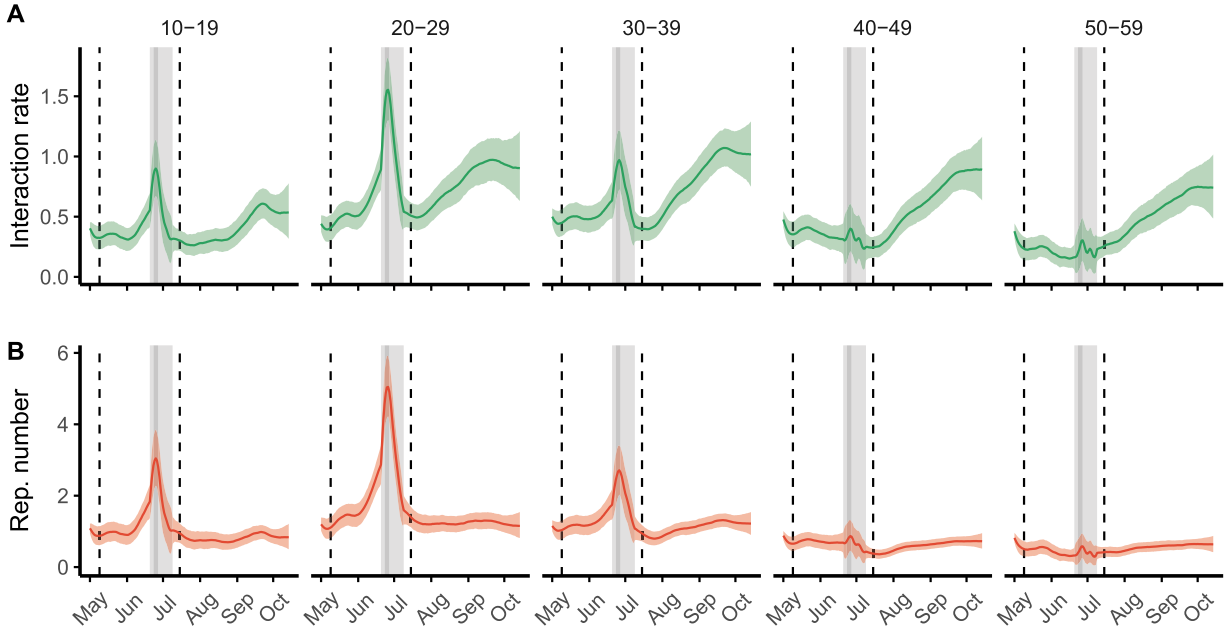

Fig. 3. Age-specific interaction rate and reproduction number. Inferred interaction rate (A) and reproduction number (B) for the age groups 10–19, 20–29, 30–39, 40–49, and 50–59 are shown. The remaining age groups are omitted here for clarity but are provided in Figs. S4-S5 of the Supplementary Information. The peaks in both the interaction rate and the reproduction number align with the Sant Joan festivities (dark grey shaded area).

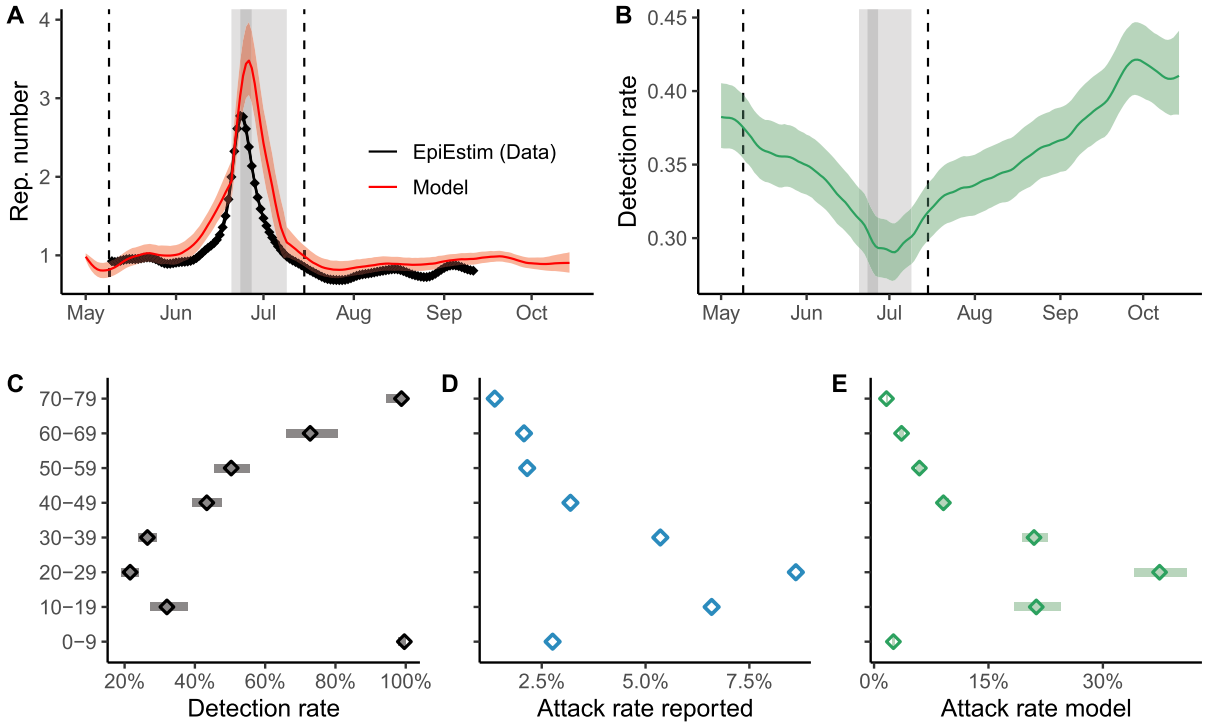

Fig. 4. Overall reproduction number, attack- and detection rates.A. The overall reproduction number as estimated by the model (red) and calculated directly from the data using EpiEstim (black). The dark grey shaded area represents the Sant Joan weekend, while the light grey shaded area marks the period when nightclubs were permitted to reopen. B. Time evolution of the overall detection rate, driven by shifts in infection patterns across different age groups. C. Age-specific attack rates derived from the model, with markers indicating median values and horizontal bars showing the 95 % credible interval (CrI). D. Same as C, but based on reported cases. E. Age-specific detection rates inferred through model calibration (see Code Availability statement).

(CrI: 27–31 %) by early July, before rising again to 41 % (CrI: 39–44 %). Notably, the rapid increase in reported cases in early July coincides with the period of the lowest detection rate.

Similar to the detection rate, the attack rate also varies significantly across age groups. The reported cases correspond to an attack rate ranging from 1.4 % for the 70–79 age group to 8.6 % for the 20–29 age group (Fig. 4D). These differences become even more pronounced when accounting for the heterogeneity in detection rates (Fig. 4E). Based on the model, the attack rate is estimated at 1.6 % (CrI: 1.5–1.7 %) for the 70–79 age group and 37 % (CrI: 34–41 %) for the 20–29 age group. These findings indicate that, between May 1st and October 15, a substantial portion of the population aged 10–40 years was infected. The precise amount depends heavily on the age-specific IHR. In the sensitivity analysis, we consider a scenario with a stronger increase in the virulence of the Delta variant, which lowers the estimated attack rate for the 20–29 age group to 27.4 % (CrI: 24.9–30.3 %).

Discussion

Our assessment of the Delta variant's transmission advantage relative to the Alpha variant is in line with previous estimations [15–18]. Nonetheless, this transmission advantage heavily depends on the generation time. As shown in the sensitivity analysis, the transmission advantage diminishes when shorter generation times are assumed for both variants. The same holds when the Delta variant is considered to have a shorter generation time than the Alpha variant, as some evidence suggests [41]. Previous studies have shown that generation time is also influenced by the NPIs in place [42]. According to the model's initialization, there were already around 30–40 active Delta variant cases by April 1st. However, the first Delta variant case was not detected until April 2022. This highlights how limited sequencing capacity—an average of 50 and a maximum of 200 samples per day—makes the early detection and prevention of a new VOC nearly impossible.

From a public health perspective, our findings indicate that a combination of three critical factors contributed to the rapid surge in case numbers: the relaxation of restrictions, the emergence of the Delta variant, and the very low vaccination coverage among younger age groups. A global reproduction number of approximately 3, and between 4 and 5 in the 20–29 age group, had only previously been observed in Spain during the first wave in spring 2020 [43]. While the Delta variant and vaccination levels can be quantified relatively easily, linking the relaxation of restrictions to increasing contact rates is more challenging. Both the data and the model reveal that the reproduction number and contact rates began to rise even before nightclubs reopened. Given the low vaccine coverage in these age groups, the increased interaction rates directly translated into a higher reproduction number. It is plausible that the combination of the end of the state of alarm, vaccine rollout, and low fatality rates in late May contributed to a general relaxation in attitudes toward SARS-CoV-2. The reopening of nightclubs may have then enabled the reproduction number to spike during the Sant Joan long weekend.

Similarly to the initial increase, the steady decline in the reproduction number following the Sant Joan long weekend does not coincide with the introduction of any specific NPIs. In fact, our findings suggest that the closure of nightclubs and the enforcement of a curfew played only a minor role in reducing the reproduction number. The initial drop can likely be attributed to the conclusion of the Sant Joan celebrations. The subsequent decline to values near 1 might be explained by heightened awareness in response to the exponentially rise in cases [44]. This hypothesis could have been validated if the evolution of contact rates were tracked in Catalonia, as it is done in Germany, for instance [45]. Real-time implementation of such monitoring programs would not only enhance our understanding of the relationship between epidemics and human

behavior [46,47], but also serve as a valuable tool for tracking the progression of the epidemic.

The trend in contact rates indicates that all age groups increased their interactions starting in mid-July, despite the curfew being in place. Unlike the surge in contact rates observed in June, the growing vaccination coverage across all age groups helped prevent a significant rise in the reproduction number. This underscores how the availability of vaccines allowed the population to resume social interactions more safely. However, one source of uncertainty is the impact of waning immunity, which the model does not account for [48,49]. For older age groups, who received their second dose between April and May, the estimated rise in contact rates in the model could potentially reflect the effects of waning immunity rather than actual changes in behavior.

The evolution of the overall detection rate illustrates how the rapidly unfolding epidemic among younger individuals posed significant challenges for health authorities in tracking its spread. Nevertheless, the detection rate remained considerably higher—approximately twice as high—compared to the first wave in spring 2020 in Spain [43,50]. With the exception of the 0–9 and 10–19 age groups, detection rates declined in accordance with the probability of developing symptoms across age groups [51]. For instance, individuals aged 70–79 were three times more likely to be detected than those aged 20–29. This highlights that monitoring an epidemic becomes increasingly challenging when it primarily affects younger individuals who are more likely to exhibit mild or no symptoms.

The significant rise in interaction rates among younger individuals is also reflected in the attack rates. According to the model, the attack rate is approximately 40 % for those aged 20–29, around 20 % for the 10–19 and 30–39 age groups, and nearly an order of magnitude lower for rest of the groups. However, estimating these attack rates involves considerable uncertainty. To account for this, in the sensitivity analysis we explored the impact of different assumptions about the increase in virulence. For scenarios with the highest assumed virulence for the Delta variant, the attack rate among the 20–29 age group drops to approximately 27 %. Nevertheless, these attack rates remain significantly higher than those observed in these age groups during the first wave in 2020 [50].

Another limitation of this study pertains to the contact patterns. In the absence of more specific data, we were required to parametrize the model using a pre-pandemic contact matrix [28]. However, the considerable fluctuations in contact rates during the studied period suggest that contact patterns likely shifted over time. Future research should seek to address this problem by integrating real-time behavioral data in the model. Furthermore, the exclusion of the 80+ age group due to the unavailability of care homes data may also have introduced a bias in the results, although, given the marginal role that the elderly population had in driving the epidemic, we find that unlikely to be significant. Other two possible shortcomings of this work are the omission of waning immunity and the absence of different types of vaccines, which should be incorporated in future works. Finally, it might be beneficial to analyze different geographical regions separately [52] or use a meta-population model incorporating individual mobility patterns [53]. Unfortunately, such data are unavailable because the Spanish government's project to track mobility using large-scale mobile phone data was discontinued on May 10. Despite this, the epidemic's evolution was remarkably consistent across all regions, suggesting that geographical aggregation provides a reasonable approximation.

Conclusion

We have demonstrated that the premature relaxation of NPIs during the spread of a new, more transmissible variant, combined with low vaccination coverage among younger individuals, resulted in a sharp surge in infections and hospitalizations. The large pool of unvaccinated individuals in the younger population drove an increase in contacts, which eventually caused a significant rise in cases and hospitalizations among older age groups as well. In contrast, when contacts rose again after vaccines became available to younger individuals, the reproduction number showed only minimal change.

While we can confidently assert that a substantial fraction of the young population was infected during the studied period, providing precise estimates remains challenging due to many sources of uncertainty, such as the age specific contact rates throughout the months under consideration. More accurate estimates of these values are crucial to estimate the real-time evolution of the epidemic as well as to perform detailed retrospective analysis.

Ethical approval

The study is exempt from ethical approval, because is not applicable.

Funding

Sponsors have had no involvement in this research study.

Author contributions

B.S. and A.A. conceived of and designed the study. G.B. built an early version of the model. B.S. carried out the numerical simulations. A.A., P.G. and C.G. analyzed the results. All authors discussed the results. B.S. wrote the first draft of the manuscript. All authors edited and approved the manuscript.

Code availability

The code for the entire analysis is available on Github https://github.com/steinegg/Catalonia_DeltaVariant.

Data availability

Case data is publicly available at Ref. [1]. The sequencing data is available together with the code on Github https://github.com/steinegg/Catalonia_DeltaVariant.

Declaration of Competing Interest

The authors declare that they have no competing financial interests or personal relationships that could have appeared to influence the work reported in this paper.

Acknowledgements

This work has been supported by Spanish Ministerio de Ciencia e Innovación (PID2021-128005NB-C21), Generalitat de Catalunya (2021SGR-00633), Universitat Rovira i Virgili (2023PFR-URV-00633) and the European Union's Horizon Europe Programme under the CREXDATA project (grant agreement no.101092749). AA acknowledges ICREA Academia, and the Joint Appointment Program at Pacific Northwest National Laboratory (PNNL). PNNL is a multi-program national laboratory operated for the U.S. Department of Energy (DOE) by Battelle Memorial Institute under Contract No.DE-AC05-76RL01830.

Appendix A. Supporting information

Supplementary data associated with this article can be found in the online version at doi:10.1016/j.jiph.2025.102771.

References

[1] Departament de Salut de la Generalitat de Catalunya. Dades COVID; 2021. ⟨https://dadescovid.cat/⟩ [Online; Accessed 19-December-2021].
[2] Pekar J, Worobey M, Moshiri N, Scheffler K, Wertheim JO. Timing the SARS-CoV-2 index case in Hubei province. Science 2021;372:412–7.
[3] Davis JT, et al. Cryptic transmission of SARS-CoV-2 and the first COVID-19 wave. Nature 2021;600:127–32.
[4] Han E, et al. Lessons learnt from easing COVID-19 restrictions: an analysis of countries and regions in Asia Pacific and Europe. Lancet 2020;396:1525–34.
[5] Zhang F, et al. Predictors of COVID-19 epidemics in countries of the World Health Organization African Region. Nat Med 2021;27:2041–7.
[6] Harvey WT, et al. SARS-CoV-2 variants, spike mutations and immune escape. Nat Rev Microbiol 2021;19:409–24.
[7] Planas D, et al. Sensitivity of infectious SARS-CoV-2 B.1.1.7 and B.1.351 variants to neutralizing antibodies. Nat Med 2021;27:917–24.
[8] Volz E, et al. Assessing transmissibility of SARS-CoV-2 lineage B.1.1.7 in England. Nature 2021;593:266–9.
[9] Davies NG, et al. Estimated transmissibility and impact of SARS-CoV-2 lineage B.1.1.7 in England. Science 2021;372:eabg3055.
[10] Kraemer MUG, et al. Spatiotemporal invasion dynamics of SARS-CoV-2 lineage B.1.1.7 emergence. Science 2021;373:889–95.
[11] Pinotti F, et al. Tracing and analysis of 288 early SARS-CoV-2 infections outside China: a modeling study. PLoS Med 2020;17:e1003193.
[12] Chinazzi M, et al. The effect of travel restrictions on the spread of the 2019 novel coronavirus (COVID-19) outbreak. Science 2020;368:395–400.
[13] Gozzi N, et al. Estimating the spreading and dominance of SARS-CoV-2 VOC 202012/01 (lineage B.1.1.7) across Europe. medRxiv 2021.
[14] Campbell F, et al. Increased transmissibility and global spread of SARS-CoV-2 variants of concern as at June 2021. Eur Surveill 2021;26:1–6.
[15] Li B, et al. Viral infection and transmission in a large, well-traced outbreak caused by the SARS-CoV-2 Delta variant. Nat Commun 2022;13:460.
[16] Alizon S, et al. Rapid spread of the SARS-CoV-2 Delta variant in some French regions, June 2021. Eur Surveill 2021;26:2100573.
[17] Tegally H, et al. Rapid replacement of the Beta variant by the Delta variant in South Africa. medRxiv 2021.
[18] Sonabend R, et al. Non-pharmaceutical interventions, vaccination, and the SARS-CoV-2 delta variant in England: a mathematical modelling study. Lancet 2021;398:1825–35.
[19] Earnest R, et al. Comparative transmissibility of SARS-CoV-2 variants Delta and Alpha in New England, USA. Cell Rep Med 2022;3:100583.
[20] Flaxman S, et al. Estimating the effects of non-pharmaceutical interventions on COVID-19 in Europe. Nature 2020;584:257–61.
[21] Haug N, et al. Ranking the effectiveness of worldwide COVID-19 government interventions. Nat Hum Behav 2020;4:1303–12.
[22] Knock ES, et al. Key epidemiological drivers and impact of interventions in the 2020 SARS-CoV-2 epidemic in England. Sci Transl Med 2021;13:eabg4262.
[23] Tregoning JS, Flight KE, Higham SL, Wang Z, Pierce BF. Progress of the COVID-19 vaccine effort: viruses, vaccines and variants versus efficacy, effectiveness and escape. Nat Rev Immunol 2021;21:626–36.
[24] Moore S, Hill EM, Tildesley MJ, Dyson L, Keeling MJ. Vaccination and non-pharmaceutical interventions for COVID-19: a mathematical modelling study. Lancet Infect Dis 2021;21:793–802.
[25] DiDomenico L, Sabbatini CE, Pullano G, Levy-Bruhl D, Colizza V. Impact of January 2021 curfew measures on SARS-CoV-2 B.1.1.7 circulation in France. Eur Surveill 2021;26:2100272.
[26] Wikipedia. Pandemia de COVID-19 a Catalunya — Wikipedia, the free encyclopedia; 2021. ⟨http://ca.wikipedia.org/w/index.php-title=Pand%C3%A8mia%20de%20COVID-19%20a%20Catalunya&oldid=28489476⟩ [Online; Accessed 27-October-2021].
[27] Wikipedia. Bonfires of Saint John. ⟨https://en.wikipedia.org/wiki/Bonfires_of_Saint_John⟩ [Online; Accessed 17-January-2022].
[28] Prem K, Cook AR, Jit M. Projecting social contact matrices in 152 countries using contact surveys and demographic data. PLoS Comput Biol 2017;13:e1005697.
[29] Bager P, et al. Risk of hospitalisation associated with infection with SARS-CoV-2 lineage B.1.1.7 in Denmark: an observational cohort study. Lancet Infect Dis 2021;21:1507–17.
[30] Sheikh A, et al. SARS-CoV-2 Delta VOC in Scotland: demographics, risk of hospital admission, and vaccine effectiveness. Lancet 2021;397:2461–2.
[31] Stan Development Team. The Stan Core Library. Version 2.21.2; 2021. ⟨http://mc-stan.org/3⟩.
[32] Stan Development Team. RStan: the R interface to Stan. R package version 2.21.2; 2020. ⟨http://mc-stan.org/⟩.
[33] Gelman A, Rubin DB. Inference from iterative simulation using multiple sequences. Stat Sci 1992;7:457–72.
[34] Arenas A, et al. Modeling the spatiotemporal epidemic spreading of COVID-19 and the impact of mobility and social distancing interventions. Phys Rev X 2020;10:041055.
[35] Cori A, Ferguson NM, Fraser C, Cauchemez S. A new framework and software to estimate time-varying reproduction numbers during epidemics. Am J Epidemiol 2013;178:1505–12.
[36] Cori A. EpiEstim: estimate time varying reproduction numbers from epidemic curves. R package version 2.2-3; 2020. ⟨https://CRAN.R-project.org/package=EpiEstim⟩.
[37] Svensson A. A note on generation times in epidemic models. Math Biosci 2007;208:300–11.
[38] Gostic KM, et al. Practical considerations for measuring the effective reproductive number, Rt. PLoS Comput Biol 2020;16:e1008409.
[39] Becker NG, Watson LF, Carlin JB. A method of non–parametric back–projection and its application to aids data. Stat Med 1991;10:1527–42.
[40] Michael Höhle D.S.B. Non-parametric back-projection of incidence cases to exposure time; 2019. ⟨https://cran.r-project.org/web/packages/BayesianTools/index.html⟩.
[41] Meng Z, et al. Transmission dynamics of an outbreak of the COVID-19 Delta Variant B.1.617.2 – Guangdong Province, China, May–June 2021. China CDC Wkly 2021;3:584.
[42] Ali ST, et al. Serial interval of SARS-CoV-2 was shortened over time by non-pharmaceutical interventions. Science 2020;369:1106–9.
[43] Steinegger B, et al. Joint analysis of the epidemic evolution and human mobility during the first wave of COVID-19 in Spain: retrospective study. JMIR Public Health Surveill 2023;9:e40514.
[44] Funk S, Gilad E, Watkins C, Jansen VAA. The spread of awareness and its impact on epidemic outbreaks. Proc Natl Acad Sci USA 2009;106:6872–7.
[45] Research Group P4 Robert Koch-Institute, Brockmann Dirk. Covid-19 mobility project; 2021. ⟨https://www.covid-19-mobility.org/contact-index/⟩.
[46] Bharti N. Linking human behaviors and infectious diseases. Proc Natl Acad Sci USA 2021;118:e2101345118.
[47] Burgio G, Steinegger B, Arenas A. Homophily impacts the success of vaccine rollouts. Commun Phys 2022;5:70.
[48] Goldberg Y, et al. Waning immunity after the BNT162b2 vaccine in Israel. N Engl J Med 2021;385:e85.
[49] Chemaitelly H, et al. Waning of BNT162b2 vaccine protection against SARS-CoV-2 infection in Qatar. N Engl J Med 2021;385:e83.
[50] Pollan M, et al. Prevalence of SARS-CoV-2 in Spain (ENE-COVID): a nationwide, population-based seroepidemiological study. Lancet 2020;396:535–44.
[51] Davies NG, et al. Age-dependent effects in the transmission and control of COVID-19 epidemics. Nat Med 2020;26:1205–11.
[52] Pullano G, et al. Underdetection of cases of COVID-19 in France threatens epidemic control. Nature 2021;590:134–9.
[53] Citron DT, et al. Comparing metapopulation dynamics of infectious diseases under different models of human movement. Proc Natl Acad Sci USA 2021;118:e2007488118.